Volume 62
Number 5
20 January 2026
Pages 1301–1656

ChemComm

Chemical Communications

rsc.li/chemcomm

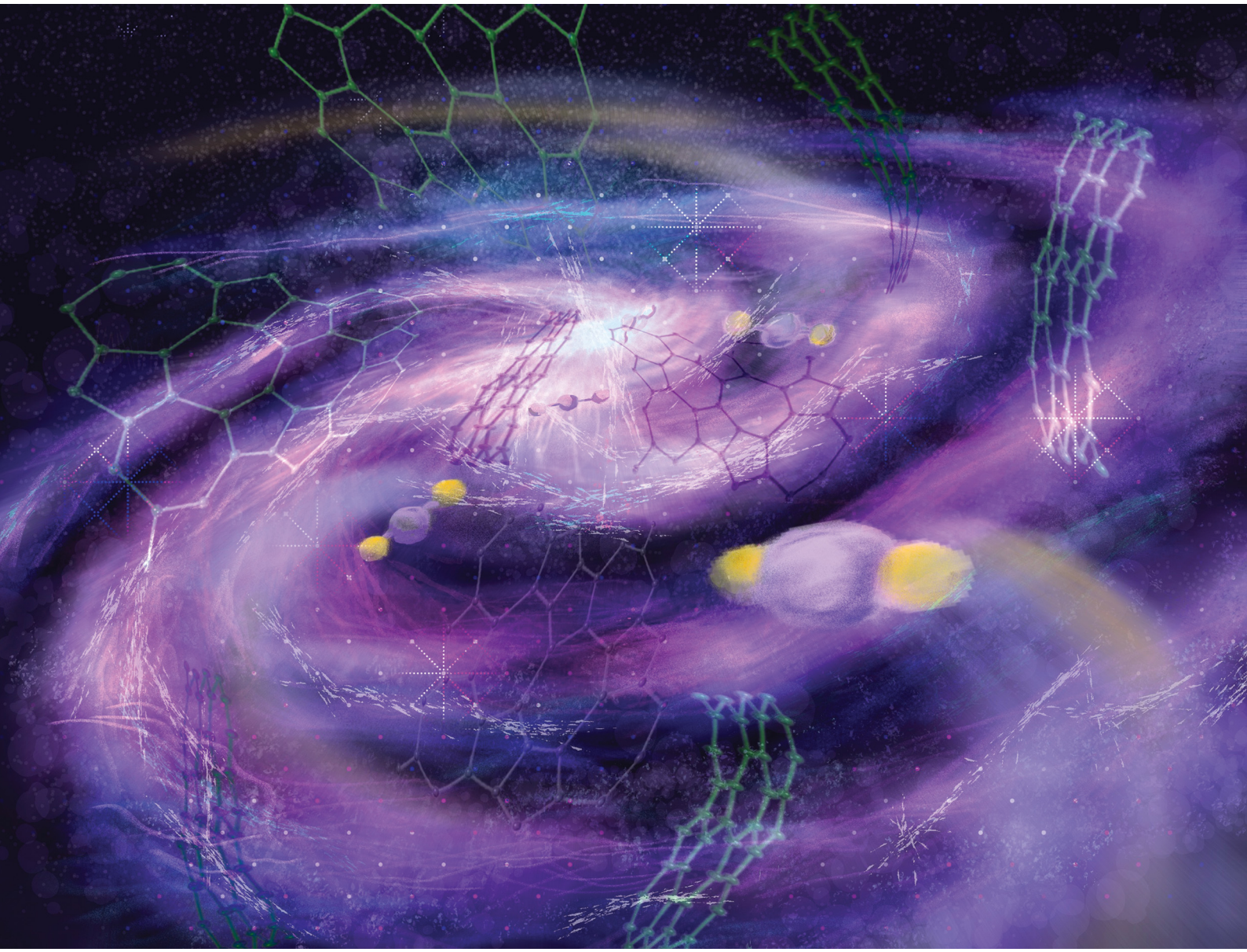

ISSN 1359-7345

ROYAL SOCIETY OF CHEMISTRY

COMMUNICATION

Georgiy Akopov *et al.*

Probing layered Y(*TM*)B_4 (*TM* = Cr, Mo and W) borides as efficient hydrogen evolution reaction electrocatalysts

ChemComm

COMMUNICATION

View Article Online
View Journal | View Issue

Cite this: *Chem. Commun.*, 2026, **62**, 1497

Received 18th November 2025,
Accepted 2nd December 2025

DOI: 10.1039/d5cc06558e

rsc.li/chemcomm

Probing layered Y(*TM*)B_4 (*TM* = Cr, Mo and W) borides as efficient hydrogen evolution reaction electrocatalysts

MD Ali Hossain, [a] Lesly Delgado, [a] Rutva Joshi,[a] Sylvie Rangan [b] and Georgiy Akopov *[a]

In this study, three layered ternary metal borides were analyzed: $YCrB_4$, $YMoB_4$, and YWB_4. YWB_4 demonstrated the highest catalytic activity, surpassing the Pt/C catalyst by 185 mV overpotential at an industrially relevant current density of 1000 mA cm^{-2}. Furthermore, stability testing revealed that YWB_4 retained 95% of its initial activity after 25 hours of continuous operation (5000 cycles) at 1000 mA cm^{-2}, underscoring its potential as a robust and sustainable HER catalyst for hydrogen production.

Due to growing public concern over limited fossil fuel reserves, environmental issues, and climate change, there has been a significant rise in interest towards sustainable and renewable energy sources.[1] Hydrogen has stood out as a highly promising solution to the global energy crisis in recent years due to its high energy density, zero-carbon emission, and eco-friendly nature, and consequently, it is viewed as a viable alternative to fossil fuels.[2–5] The industrial generation of hydrogen from fossil fuels, which releases CO_2 alongside H_2, is inconsistent with the principles of sustainable development in today's society and economy.[6] Water splitting powered by renewable resources is regarded as one of the most promising technologies.[7,8] Electrochemical and photoelectrochemical processes are the two leading methods for water splitting.[9] Practically, electrocatalysis is preferred over photocatalysis due to its superior efficiency.[10] Recently, water electrolysis has attracted significant interest as a method for hydrogen production. This process involves using electrical energy to split water into hydrogen (*via* the hydrogen evolution reaction, HER) and oxygen (*via* the oxygen evolution reaction, OER), making it a promising approach for generating hydrogen using renewable energy sources.[11–13] Electrocatalysts are crucial for efficiently producing hydrogen and minimizing the overpotential in water electrolysis. Platinum group metals are recognized as the most efficient electrocatalysts for the HER, offering low overpotentials.[14] Due to their high cost and limited availability, their applications remain restricted.[15] Consequently, developing highly efficient, low-cost HER electrocatalysts to replace Pt-based materials is crucial for large-scale hydrogen production.

Bulk metal borides have recently attracted attention for their remarkable properties, such as superhardness,[16] thermoelectric behavior,[17] magnetic characteristics[18,19] and potential solid-state fuels.[20] In recent years, compounds derived from earth-abundant transition metals have gained significant research attention because of their affordability and widespread availability.[21,22] Some transition-metal-derived materials found to be more active and stable for the HER are transition metal alloys (TMAs),[13] dichalcogenides (TMDs),[23] nitrides (TMNs)[24] and carbides (TMCs).[25] In recent times, transition metal borides like Mo-B (in both bulk and nanoscale forms),[26–30] MoAlB (bulk),[31] Co-B (amorphous),[32,33] Ni-B (amorphous and nanoscale),[34] Co-Ni-B (amorphous),[35] and FeB_2 (nanoscale)[9] have emerged as promising HER electrocatalysts. This is attributed to their abundance, cost-effectiveness, and excellent HER performance and stability in acidic and alkaline environments. Metal borides, compared to metal carbides, sulphides, and phosphides, exhibit better HER activity (Table S3). Although these materials are superior at low current densities, they underperform at high current densities (Table S3).

In recent years, molybdenum-based materials like molybdenum disulfide,[36] molybdenum carbide,[37] and molybdenum phosphides[38] have been widely studied as cost-effective alternative electrocatalysts for the hydrogen evolution reaction (HER). Although molybdenum and tungsten share similar chemical and physical properties, tungsten-based materials have been significantly less explored than molybdenum. For instance, tungsten disulfide,[39] carbides,[40] and phosphides[41] demonstrate comparable or even superior HER activity relative to their molybdenum analogues. Nevertheless, tungsten-based borides have not yet been explored. Chromium belongs to the

[a] *Department of Chemistry, Rutgers University, Newark, Newark, NJ 07102, USA. E-mail: georgiy.akopov@rutgers.edu*
[b] *Department of Physics and Astronomy and Laboratory for Surface Modification, Rutgers University – New Brunswick, Piscataway, NJ 08854, USA*

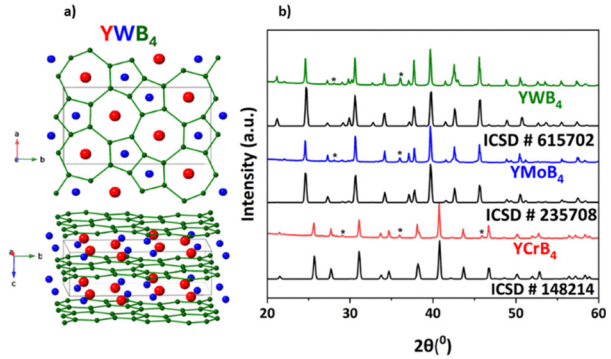

Fig. 1 (a) Crystal structure of YWB_4, (b) powder X-ray diffraction patterns for $YCrB_4$, $YMoB_4$, and YWB_4. Reference patterns: ICSD 148214,[45] 235708,[46] and 615702,[43] respectively. (*) – peaks for YB_4.

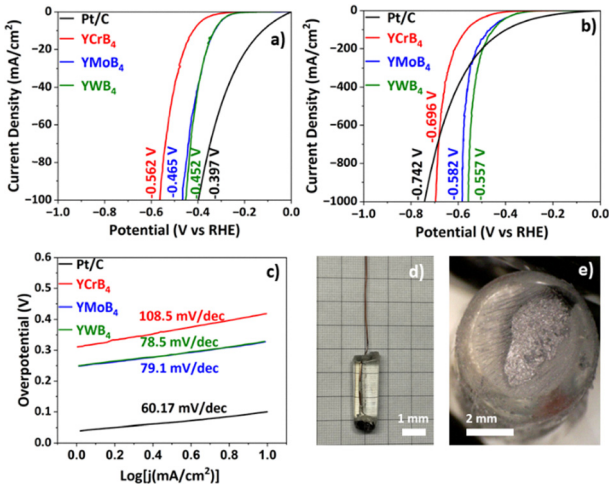

Fig. 2 (a) Polarization curves of 20% Pt/C, $YCrB_4$, $YMoB_4$, and YWB_4 measured in 0.5 M H_2SO_4. (b) Polarization curves showing high current density behaviours of 20% Pt/C, $YCrB_4$, $YMoB_4$, and YWB_4. (c) The corresponding Tafel plots of 20% Pt/C, $YCrB_4$, $YMoB_4$, and YWB_4. (IR-drop was compensated.) (d) Working electrode assembly after polishing on sandpaper. (e) Electrode surface of YWB_4.

same group in the periodic table as molybdenum and tungsten, and therefore shares specific chemical characteristics, including the ability to form similar compounds with boron.[42]

In this study, the successful synthesis of $YCrB_4$, $YMoB_4$, and YWB_4 analogues was presented; among these, YWB_4 exhibits excellent HER activity and high current density performance. These materials were prepared *via* arc-melting, following the method detailed in the SI. Briefly, high-purity yttrium, chromium, molybdenum, tungsten, and boron powders were weighed in the Y : M : B = 1 : 1 : 4.25 stoichiometric ratios (totalling 0.75 g), compacted into pellets, and then arc-melted under an argon atmosphere. Optimizing arc-melting parameters, particularly the applied current, was determined to be a critical step for the successful synthesis of the desired phases (SI). The synthesized materials were characterized using powder X-ray diffraction (PXRD) (Fig. 1). Fig. 1a depicts the crystal structures of YWB_4 (*Pbam*, ICSD 615702).[43] This crystal structure is similar to AlB_2, with both being layered with alternating layers of boron and metal. However, in AlB_2 the boron atoms are arranged in sheets of hexagons, while in YWB_4 the boron atoms are arranged in 7- (accommodating Y) and 5-membered rings (accommodating Cr, Mo, and W metals). This is due to the difference in radii of Y (180 pm) and other transition metals (Cr – 140 pm, Mo – 145 pm, and W – 135 pm).[44] The bond lengths of the three crystal structures are listed in Table S1, and they follow the trend of the atomic radii for the three metals (increasing from Cr to Mo and decreasing for W). The bond length correlates with the activity seen for the Cr, Mo and W cases, suggesting that an optimal bond length can be achieved through solid-solution formation that would further enhance the performance. Fig. 1b presents the powder X-ray diffraction patterns for all three compounds. Each target phase was successfully formed with more than 95% weight purity, although a minor impurity phase (YB_4) was also detected. Pure YB_4 showed essentially no catalytic activity (Fig. S2) and as such does not contribute to the activity of the main phase.

The electrochemical hydrogen evolution reaction (HER) activity of the ternary borides $YCrB_4$, $YMoB_4$, and YWB_4 has been investigated for the first time. Electrochemical measurements were conducted in a conventional three-electrode setup using 0.5 M H_2SO_4 as the electrolyte, with a scan rate of 5 mV s^{-1} and an IR compensation applied (Fig. 2). The working electrodes consisted of polished arc-melted ingots mounted in epoxy and attached to copper wire (details in the SI). As shown in the polarization curves in Fig. 2a, YWB_4 exhibited the lowest overpotential of 452 mV to reach a current density of 100 mA cm^{-2}, outperforming both $YCrB_4$ and $YMoB_4$. This establishes YWB_4 as a highly efficient HER catalyst, with its overpotential being 110 mV lower than that of $YCrB_4$ (562 mV) at 100 mA cm^{-2}. Under high current densities of 1000 mA cm^{-2}, the overpotential difference increases to 139 mV compared to $YCrB_4$ (Fig. 2b). Notably, when the current density exceeds the industrial benchmark of 300 mA cm^{-2},[47] it not only further increases the overpotential difference between YWB_4 and $YCrB_4$ (Fig. 2b), but also provides a superior performance of about 25% over the self-tested Pt/C. A comparison of the samples studied in this paper with other reported metal borides is presented in Table S3. The mechanism of the catalytic process and the nature of the active sites are currently under investigation through a computational collaboration.

The Tafel plot is commonly used to show the catalytic mechanism of the hydrogen evolution reaction (HER). In general, three fundamental steps can serve as the rate-determining step (RDS): the Volmer step (electrochemical hydrogen ion adsorption, Tafel slope $\approx$120 mV dec^{-1}), the Heyrovsky step (electrochemical desorption, $\approx$40 mV dec^{-1}), and the Tafel step (chemical desorption, $\approx$30 mV dec^{-1}). The experimentally determined Tafel slopes for $YCrB_4$, $YMoB_4$, and YWB_4 are 108.5 mV dec^{-1}, 79.1 mV dec^{-1}, and 78.5 mV dec^{-1}, respectively (Fig. 2c). These values fall within a range of 78.5–108.5 mV dec^{-1}, which does not correspond precisely to any of the ideal theoretical slopes. This indicates the complexity of the HER mechanism on these bulk catalysts and makes it

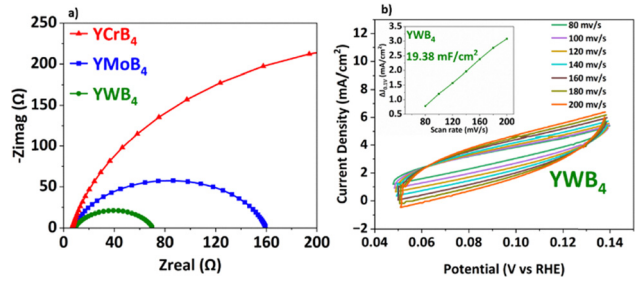

Fig. 3 (a) Electrochemical impedance spectroscopy (EIS) Nyquist plots of $YCrB_4$, $YMoB_4$, and YWB_4. (b) Cyclic voltammetry curve of YWB_4. (Inset showing the difference in the current density of ΔJ ($J_a - J_c$) at 0.1 V *vs.* RHE plotted against the scan rate is fitted to a linear regression to estimate C_{dl}.)

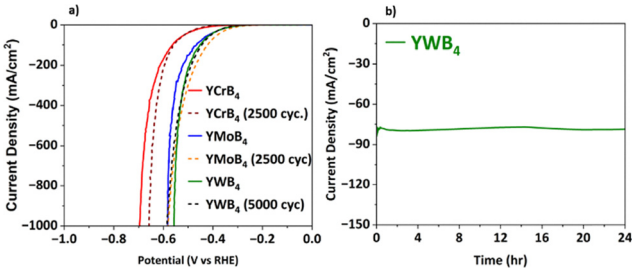

Fig. 4 (a) Polarization curve of $YCrB_4$, $YMoB_4$, and YWB_4 before and after 2500, 2500, and 5000 cycles, respectively. (b) Chronoamperometry curve of YWB_4 for 24 h.

challenging to identify the RDS from Tafel analysis alone. Nonetheless, YWB_4 displays the smallest Tafel slope, indicating a more rapid and efficient HER process compared to the other boride samples. Fig. 2d and Fig. 2e represent the working electrode assembly after polishing on sandpaper and the electrode surface of YWB_4, respectively.

As shown in Fig. 3a, the solution resistance (R_s) that was used for IR-drop compensation was nearly identical for all samples, attributed to the consistent electrode preparation method. The Nyquist plots for each sample were fitted using an equivalent circuit model incorporating a constant phase element (CPE). The excellent HER performance of YWB_4 can be linked to its high electrochemically active surface area (ECSA). The ECSA of YWB_4 is shown in Fig. 3b and estimated by determining its double-layer capacitance (C_{dl}) using cyclic voltammetry (CV) at scan rates ranging from 80 to 200 mV s^{-1} in the non-faradaic region (0.05–0.15 V *vs.* RHE).[42] YWB_4 exhibited a C_{dl} value of 19.38 mF cm^{-2}, which exceeds several previously reported values,[28,42,48] further highlighting its superior catalytic activity.

X-ray photoelectron spectroscopy (XPS) data were collected to investigate the surface composition of $YCrB_4$, $YMoB_4$, and YWB_4 before and after electrocatalysis (Fig. S4–S12). The starting surfaces indicate typical metal boride features, with a thin oxide/hydroxide formation upon exposure to air. Metallic features are clearly derived from the asymmetry of the boride core levels. After electrocatalysis, a thicker oxide/hydroxide layer of similar composition as the initial surface is measured. The SEM–EDS characterization (Fig. S13–S15) and XPS data (Table S1) confirm the uniform distribution of Y, transition metals (Cr, Mo, W), and B in $YCrB_4$, $YMoB_4$, and YWB_4. The obtained atomic ratios closely match the desired stoichiometric ratios, confirming homogeneous mixing and successful formation of the desired borides.

Catalyst stability and durability are essential factors for real-world applications, particularly in acidic media. To evaluate these characteristics, comprehensive tests were conducted on the Y(*TM*)B_4 electrodes. Long-term stability was assessed *via* cyclic voltammetry over 2500 (≈12.5 hours) to 5000 cycles (≈25 hours) for $YCrB_4$, $YMoB_4$, and YWB_4 at a high current density of 1000 mA cm^{-2}. As illustrated in Fig. 4a, the post-test polarization curve showed only a slight deviation for all the electrodes, with the YWB_4 electrode retaining a high percentage (95%) of its initial catalytic activity. Durability was further examined for YWB_4 through a continuous electrolysis experiment (chronoamperometry) at a constant current density of approximately 80 mA cm^{-2} for 24 hours. As shown in Fig. 4b, the current density remained nearly unchanged, indicating excellent durability. These findings demonstrate that YWB_4 exhibits outstanding stability and durability under extended, industrial scale operating conditions, making it a strong candidate for sustainable hydrogen production in harsh environments.

In conclusion, the ternary metal borides $YCrB_4$, $YMoB_4$, and YWB_4 were successfully synthesized *via* arc melting, characterized, and evaluated for their hydrogen evolution reaction (HER) performance in a highly acidic environment for the first time. Among them, YWB_4 demonstrated the highest HER activity, outperforming both its counterparts and even surpassing the performance of the commercial Pt/C catalyst at elevated current densities. Additionally, YWB_4 exhibited remarkable long-term stability and durability, with negligible loss in HER activity after 5000 cycles and 25 hours of continuous operation in an acidic electrolyte. These findings highlight the significant potential of boride-based materials as promising HER electrocatalysts for future sustainable hydrogen production.

This manuscript is dedicated in loving memory of a dear friend Rebecca Lin Li. This research was supported by a Rutgers University, Newark startup grant (A. H., L. D., R. J., G. A.). The X-ray diffractometer was purchased with support from the National Science Foundation Grant No. [2018753]. L. D. was supported by the Rutgers University – Newark Dean's 2024 Summer Undergraduate Research Fellowship (SURF). Supplement funding for this project was provided by the Rutgers University – Newark Chancellor's Research Office (A. H.). This research was supported by a Rutgers University Research Council Award (L. D. and G. A.). This work was supported by the donors of ACS Petroleum Research Fund under ACS PRF Doctoral New Investigator Grant 68959-DNI10 (A. H. and G. A.). The authors acknowledge the Laboratory for Surface Modifications facilities for XPS analysis.

Conflicts of interest

There are no conflicts to declare.

Data availability

The data supporting this article have been included as part of the supplementary information (SI). Supplementary information: details of synthesis and characterization of the metal borides. See DOI: https://doi.org/10.1039/d5cc06558e.

References

1 N. Armaroli and V. Balzani, *Angew. Chem., Int. Ed.*, 2007, **46**(1–2), 52–66.
2 C. Liu, F. Li, L.-P. Ma and H.-M. Cheng, *Adv. Mater.*, 2010, **22**(8), E28–E62.
3 K. Mazloomi and C. Gomes, *Renewable Sustainable Energy Rev.*, 2012, **16**(5), 3024–3033.
4 M. G. Walter, E. L. Warren, J. R. McKone, S. W. Boettcher, Q. Mi, E. A. Santori and N. S. Lewis, *Chem. Rev.*, 2010, **110**(11), 6446–6473.
5 J. A. Turner, *Science*, 2004, **305**(5686), 972–974.
6 S. Anantharaj, S. R. Ede, K. Sakthikumar, K. Karthick, S. Mishra and S. Kundu, *ACS Catal.*, 2016, **6**(12), 8069–8097.
7 Z. W. Seh, J. Kibsgaard, C. F. Dickens, I. Chorkendorff, J. K. Nørskov and T. F. Jaramillo, *Science*, 2017, **355**(6321), eaad4998.
8 A. Kudo and Y. Miseki, *Chem. Soc. Rev.*, 2008, **38**(1), 253–278.
9 I. Roger, M. A. Shipman and M. D. Symes, *Nat. Rev. Chem.*, 2017, **1**(1), 1–13.
10 Q. Lu, Y. Yu, Q. Ma, B. Chen and H. Zhang, *Adv. Mater.*, 2016, **28**(10), 1917–1933.
11 C. G. Morales-Guio, L.-A. Stern and X. Hu, *Chem. Soc. Rev.*, 2014, **43**(18), 6555–6569.
12 D. Merki and X. Hu, *Energy Environ. Sci.*, 2011, **4**(10), 3878–3888.
13 M. Zeng and Y. Li, *J. Mater. Chem. A*, 2015, **3**(29), 14942–14962.
14 C. C. L. McCrory, S. Jung, I. M. Ferrer, S. M. Chatman, J. C. Peters and T. F. Jaramillo, *J. Am. Chem. Soc.*, 2015, **137**(13), 4347–4357.
15 X. Zou and Y. Zhang, *Chem. Soc. Rev.*, 2015, **44**(15), 5148–5180.
16 G. Akopov, H. Yin, I. Roh, L. E. Pangilinan and R. B. Kaner, *Chem. Mater.*, 2018, **30**(18), 6494–6502.
17 G. Akopov, W. H. Mak, D. Koumoulis, H. Yin, B. Owens-Baird, M. T. Yeung, M. H. Muni, S. Lee, I. Roh, Z. C. Sobell, P. L. Diaconescu, R. Mohammadi, K. Kovnir and R. B. Kaner, *J. Am. Chem. Soc.*, 2019, **141**(22), 9047–9062.
18 B. P. T. Fokwa, *Encyclopedia of Inorganic and Bioinorganic Chemistry*, John Wiley & Sons, Ltd, 2014; pp 1–14.
19 G. Akopov, M. T. Yeung and R. B. Kaner, *Adv. Mater.*, 2017, **29**(21), 1604506.
20 J. T. Doane, G. M. John, A. Kolakji, A. A. Rosenberg, Y. Zhang, A. A. Chen and M. T. Yeung, *J. Am. Chem. Soc.*, 2025, **147**(19), 16578–16584.
21 M. C. Weidman, D. V. Esposito, Y.-C. Hsu and J. G. Chen, *J. Power Sources*, 2012, **202**, 11–17.
22 E. Lee and B. P. T. Fokwa, *Acc. Chem. Res.*, 2022, **55**(1), 56–64.
23 G. Zhu, J. Liu, Q. Zheng, R. Zhang, D. Li, D. Banerjee and D. G. Cahill, *Nat. Commun.*, 2016, **7**(1), 13211.
24 W.-F. Chen, J. T. Muckerman and E. Fujita, *Chem. Commun.*, 2013, **49**(79), 8896–8909.
25 Y. Zhong, X. Xia, F. Shi, J. Zhan, J. Tu and H. J. Fan, *Adv. Sci.*, 2016, **3**(5), 1500286.
26 X. Wang, G. Tai, Z. Wu, T. Hu and R. Wang, *J. Mater. Chem. A*, 2017, **5**(45), 23471–23475.
27 H. Vrubel and X. Hu, *Angew. Chem., Int. Ed.*, 2012, **51**(51), 12703–12706.
28 H. Park, A. Encinas, J. P. Scheifers, Y. Zhang and B. P. T. Fokwa, *Angew. Chem. Int. Ed.*, 2017, **56**(20), 5575–5578.
29 P. R. Jothi, Y. Zhang, J. P. Scheifers, H. Park and B. P. T. Fokwa, *Sustainable Energy Fuels*, 2017, **1**(9), 1928–1934.
30 H. Park, Y. Zhang, J. P. Scheifers, P. R. Jothi, A. Encinas and B. P. T. Fokwa, *J. Am. Chem. Soc.*, 2017, **139**(37), 12915–12918.
31 L. T. Alameda, C. F. Holder, J. L. Fenton and R. E. Schaak, *Chem. Mater.*, 2017, **29**(21), 8953–8957.
32 Z. Chen, Q. Kang, G. Cao, N. Xu, H. Dai and P. Wang, *Int. J. Hydrogen Energy*, 2018, **43**(12), 6076–6087.
33 S. Gupta, N. Patel, A. Miotello and D. C. Kothari, *J. Power Sources*, 2015, **279**, 620–625.
34 M. Zeng, H. Wang, C. Zhao, J. Wei, K. Qi, W. Wang and X. Bai, *ChemCatChem*, 2016, **8**(4), 708–712.
35 N. Xu, G. Cao, Z. Chen, Q. Kang, H. Dai and P. Wang, *J. Mater. Chem. A*, 2017, **5**(24), 12379–12384.
36 J. Kibsgaard, Z. Chen, B. N. Reinecke and T. F. Jaramillo, *Nat. Mater.*, 2012, **11**(11), 963–969.
37 W.-F. Chen, C.-H. Wang, K. Sasaki, N. Marinkovic, W. Xu, J. T. Muckerman, Y. Zhu and R. R. Adzic, *Energy Environ. Sci.*, 2013, **6**(3), 943–951.
38 P. Xiao, M. A. Sk, L. Thia, X. Ge, R. J. Lim, J.-Y. Wang, K. H. Lim and X. Wang, *Energy Environ. Sci.*, 2014, **7**(8), 2624–2629.
39 D. Voiry, H. Yamaguchi, J. Li, R. Silva, D. C. B. Alves, T. Fujita, M. Chen, T. Asefa, V. B. Shenoy, G. Eda and M. Chhowalla, *Nat. Mater.*, 2013, **12**(9), 850–855.
40 S. Wirth, F. Harnisch, M. Weinmann and U. Schröder, *Appl. Catal., B*, 2012, **126**, 225–230.
41 J. M. McEnaney, J. C. Crompton, J. F. Callejas, E. J. Popczun, C. G. Read, N. S. Lewis and R. E. Schaak, *Chem. Commun.*, 2014, **50**(75), 11026–11028.
42 H. Park, E. Lee, M. Lei, H. Joo, S. Coh and B. P. T. Fokwa, *Adv. Mater.*, 2020, **32**(28), 2000855.
43 P. Rogl, *Mater. Res. Bull.*, 1978, **13**(5), 519–523.
44 J. C. Slater, *J. Chem. Phys.*, 1964, **41**(10), 3199–3204.
45 M. Tokuda, K. Yubuta, T. Shishido and K. Sugiyama, *Acta Crystallogr., Sect. E: Crystallogr. Commun.*, 2023, **79**(11), 1072–1075.
46 C. Benndorf, M. De Oliveira, C. Doerenkamp, F. Haarmann, T. Fickenscher, J. Kösters, H. Eckert and R. Pöttgen, *Dalton Trans.*, 2019, **48**(3), 1118–1128.
47 K. Zeng and D. Zhang, *Prog. Energy Combust. Sci.*, 2010, **36**(3), 307–326.
48 S. B. Kim, J. A. Yapo, A. Yasuhara, K. Yubuta and B. P. T. Fokwa, *Small*, 2025, **21**, 2412693.

